Towards a generic control-oriented model for HEV predictive energy management

Nicoleta Stroe, Guillaume Colin, Karim Ben-Cherif, Sorin Olaru, Yann Chamaillard

Towards a generic control-oriented model for HEV predictive energy management

Nicoleta Stroe [*,**,***] **Guillaume Colin** [**] **Karim Ben-Cherif** [*]
Sorin Olaru [***] **Yann Chamaillard** [**]

[*] *Renault SAS, Lardy, France, (e-mail:{nicoleta − alexandra.stroe, karim.ben − cherif}@renault.com)*
[**] *PRISME Laboratory, Orléans University, France, (e-mail:{guillaume.colin, yann.chamaillard}@univ-orleans.fr)*
[***] *Laboratory of Signals and Systems, CentraleSupélec-CNRS-Univ. Paris-Sud, Univ. Paris-Saclay, Gif-sur-Yvette, 91192*

Abstract: The increased interest in model-based control techniques for the energy management of hybrid electric vehicles has led to a focus on generic modeling in order to allow an effective integration in model-based design procedures. An architecture-free model ensures modularity with a view to control design. Under mild assumptions, a generic model for the torque and the rotational speed of a hybrid electric vehicle is proposed in this article. In addition, the mathematical formulation of the fuel consumption minimization and the intrinsic problem of torque split are addressed. In order to illustrate its ability to handle the constraints, a model predictive control formulation is presented and applied to a dual-clutch transmission hybrid architecture.

Keywords: hybrid electric vehicle, generic model, energy management, MPC

1. INTRODUCTION

In recent years, stringent CO_2 emission regulations, as well as the depletion of fossil fuel resources have triggered a determined orientation toward alternative transportation technologies, such as hybrid electric vehicles (HEV).

For HEV, one of the most challenging problems concerning fuel consumption optimization is computation of the torque split between the engine and the motor. In the literature several techniques have been proposed: dynamic programming, which provides the global optimum, under the assumption of perfect information(Sundstrom et al., 2008), rule-based (Goerke et al., 2015), ECMS - *Equivalent Consumption Minimization Strategy* (Sciaretta et al., 2004) and its variations: A-ECMS (Musardo et al., 2005), T-ECMS (Sciarretta et al., 2004); fuzzy, genetic algorithms, game theory, deterministic Model Predictive Control (MPC) (Cairano et al., 2011), (Borhan et al., 2012), (Lu et al., 2013) and stochastic MPC (Ripaccioli et al., 2010), (Josevski and Abel, 2014). The ability to cope with constraints and also the possibility nowadays to collect information about the future speed and road profile have made the latter a very attractive method.

Model-based methods have drawn attention due to the inherent robustness of the solution, but they depend on the powertrain architecture, i.e. electric machine position and transmission type. In Rizzoni et al. (1999) a generalized model for HEV components and energy flow was proposed and in Chen et al. (2009) a global model for different vehicle types (conventional, hybrid, electric) was described, but the functional modes for each configuration were not detailed. The torque values at different levels (wheel, gearbox, crankshaft) and rotational speed of components are mandatory for a supervisory control and in the absence of a comprehensive parameterization, the control would have to be adapted for each particular configuration. In this paper, a generic control-oriented model is proposed, that will complete the HEV architecture description and will also make a contribution from a control point of view.

The improvements in fuel consumption by the use of telemetry data have been the object of several publications, such as (Kim et al., 2008) or (Manzie et al., 2012). In the former, a maximum headway of 400 m was tested, whereas in the latter the prediction was specified on a time headway, with optimal values found to be on the order of 30 s. However, within the use of the MPC method, smaller prediction horizon values are used, mostly below 20 s.

In this paper, the velocity profile and the gear engaged are assumed known in advance for a given time horizon and therefore, only the torque split problem will be addressed.

For a charge sustaining operation, a state-of-charge (SOC) balance condition is usually imposed; appropriate penalty factors can solve this problem, but they depend on the driving cycle characteristics. MPC final state constraints can lead to conservative results for short prediction horizons, as SOC varies in a small range. In this respect, the present paper proposes a new approach, that uses distance-varying limits for SOC, enforcing the convergence to the initial value, as the vehicle reaches its destination.

The article is organized as follows: first, a generic model with the associated assumptions, equations and configurations will be presented and validated on a case-study architecture. In the second part, the MPC - based energy

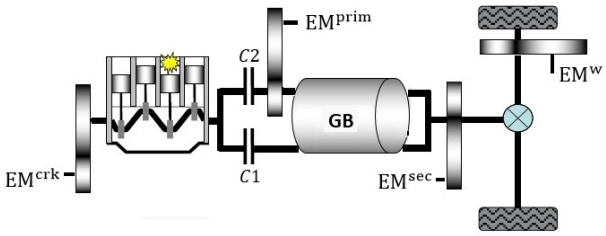

Fig. 1. Generic representation of a hybrid electric powertrain

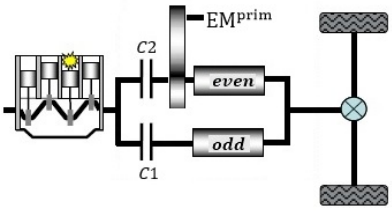

Fig. 2. Configuration (2)

management problem will be formulated; the simulation results obtained and the conclusions complete the paper.

NOTATIONS

- ICE - internal combustion engine
- EM - electric machine
- DCT - dual-clutch transmission
- R_i - gear ratio engaged on ith shaft (includes neutral definition), $i \in \{1 : odd, 2 : even\}$
- C_i - clutch status (0 - open, 1 - closed)
- $N_i = min(R_i, 1)$ - used to define the case where one of the shafts is decoupled
- FD_{R_i} - axle ratio corresponding to ith shaft
- *crk, prim, sec, w* - crankshaft, primary, secondary and wheel, respectively
- rat_{EM}^{pos} - ratio between the EM and the corresponding shaft where it is connected (*pos* - position)
- r_{ICE}^{pos} - ratio between the ICE torque at *pos* level and the ICE torque at crankshaft
- $r_{EM}^{w/pos}$ - ratio from the EM placed at *pos* to the wheel
- ω_{ICE}^{ctrl} - engine speed for a series architecture; for the others: idle speed or 0 rpm, in case of engine stop
- R_w - wheel radius

2. GENERIC HEV CONTROL-ORIENTED MODEL

The proposed model aims to cover a large class of HEV architectures under the following assumptions:

(i) potential EM connected to the crankshaft, primary shaft, secondary shaft and to the wheel, as in Fig. 1
(ii) one battery
(iii) one gear-shaft EM (an EM to the either odd or even shaft, but not both - for a dual-clutch transmission). The notation conventions assign the shaft index *2* to the EM connected to the primary. If the EM is connected to the odd shaft, the indexes will be switched.
(iv) gear and clutch dynamic not considered
(v) gear efficiency dependent only on rotational speed

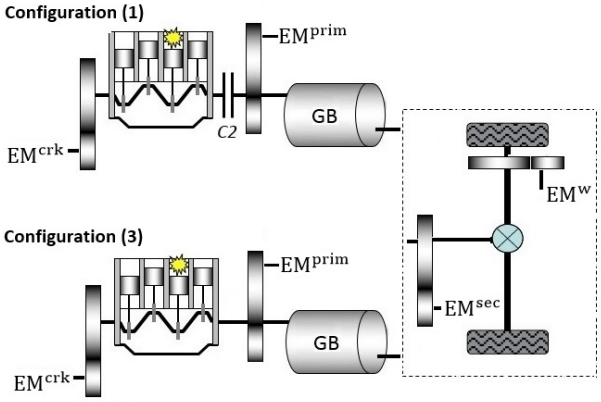

Fig. 3. Configuration (1) and (3): schematic representation

First, a parallel architecture will be considered and subsequently it will be shown that the model can be employed for other architectures. Recall also that in Chapter 4 of Guzzella and Sciarretta (2007) the power-split case was treated and a very compact model was proposed in the form:

$$\begin{bmatrix} T_f \\ T_g \end{bmatrix} = M^T \begin{bmatrix} T_{ice} \\ T_m \end{bmatrix}, \begin{bmatrix} \omega_{ice} \\ \omega_{mot} \end{bmatrix} = M \begin{bmatrix} \omega_f \\ \omega_g \end{bmatrix}, \quad (1)$$

where *f, g, mot* stand for *final driveline, generator* and *motor*, respectively. In what follows, it will be shown that our proposed model integrates and extends (1).

2.1 Model configuration

As depicted in Fig. 1, the EM position determines at least 4 possible configurations (*crk, prim, sec, w*, but also combinations: *crk* and *w*, *crk* and *prim/sec*), whereas the clutch determines 3 possible configurations:

(1) one-clutch (EM everywhere), as in Fig. 3, top
(2) dual-clutch (particular case for EM connected to the primary shaft, as in Fig. 2)
(3) no clutch (EM everywhere), as in Fig. 3, bottom

Table 1 gives a description of these configurations, with EM connected to $\overline{pos} \subseteq \{crk, prim, sec, w\}$. This implies that for $pos \notin \overline{pos}, rat_{EM}^{pos} = 0$.

Table 1. Architectures description, EM connected to $\overline{pos}$

Configuration	Description
1	$C_1 = 0, C_2 \in \{0, 1\}$
2	$C_1, C_2 \in \{0, 1\}, prim \in \overline{pos}$
3	$C_1 = 0, C_2 = 1$

2.2 Torque and rotational speed expressions

From an energy management point of view, the torque expression at the wheel level includes the complete information about a HEV architecture (EM position and gearbox). For a detailed characterization, the equations below describe the relationship between the components torque and the torque delivered at the 4 shafts (*crk, prim, sec, w*) and also the rotational speeds, as functions of the vehicle speed (v) and ω_{ICE}^{ctrl}.

$$T_w = r^w_{ICE} T_{ICE} + \sum_{pos} r^{w/pos}_{EM} T^{pos}_{EM} \quad (2)$$

with $pos \in \{crk, prim, sec, w\}$

$$\begin{bmatrix} T_{crk} \\ T_{prim} \\ T_{sec} \\ T_w \end{bmatrix} = A_T \begin{bmatrix} T_{ICE} \\ T^{crk}_{EM} \\ T^{prim}_{EM} \\ T^{sec}_{EM} \\ T^{w}_{EM} \end{bmatrix}, \begin{bmatrix} \omega_{ICE} \\ \omega^{crk}_{EM} \\ \omega^{prim}_{EM} \\ \omega^{sec}_{EM} \\ \omega^{w}_{EM} \end{bmatrix} = A_\omega \begin{bmatrix} v\dfrac{1}{R_w} \\ \omega^{ctrl}_{ICE} \end{bmatrix} \quad (3)$$

$$A_T = \begin{bmatrix} 1 & rat^{crk}_{EM} & 0 & 0 & 0 \\ r^{prim}_{ICE} & r^{prim/crk}_{EM} & rat^{prim}_{EM} & 0 & 0 \\ r^{sec}_{ICE} & r^{sec/crk}_{EM} & r^{sec/prim}_{EM} & rat^{sec}_{EM} & 0 \\ r^{w}_{ICE} & r^{w/crk}_{EM} & r^{w/prim}_{EM} & r^{w/sec}_{EM} & rat^{w}_{EM} \end{bmatrix} \quad (4)$$

$$A_\omega = \begin{bmatrix} r^w_{ICE} & 1 - C_1 - N_2 C_2 \\ r^{w/crk}_{EM} & rat^{crk}_{EM}\left(1 - C_1 - N_2 C_2\right) \\ r^{w/prim}_{EM} & rat^{prim}_{EM} C_2 \left(1 - C_1\right)\left(1 - N_2\right) \\ r^{w/sec}_{EM} & 0 \\ rat^{w}_{EM} & 0 \end{bmatrix} \quad (5)$$

$$r^{prim}_{ICE} = C_1 + C_2 - C_1 C_2 \quad (6)$$

$$r^{sec}_{ICE} = R_1 C_1 + R_2 C_2 \quad (7)$$

$$r^{w}_{ICE} = FD_{(R_1)} R_1 C_1 + FD_{(R_2)} R_2 C_2 \quad (8)$$

$$r^{pos/crk}_{EM} = r^{pos}_{ICE} rat^{crk}_{EM}, \quad pos \in \{prim, sec, w\} \quad (9)$$

$$r^{sec/prim}_{EM} = \left(R_1 C_1 C_2 + R_2\right) rat^{prim}_{EM} \quad (10)$$

$$r^{w/prim}_{EM} = FD_{(R_1 C_1 C_2 + R_2)} r^{sec/prim}_{EM} \quad (11)$$

$$r^{w/sec}_{EM} = FD_{(sec)} rat^{sec}_{EM}, \quad r^{w/w}_{EM} = rat^{w}_{EM} \quad (12)$$

These are the static relationships which have to be considered in conjunction with the dynamic part of the model represented by the state-of-charge, for which an equivalent circuit model is used (OCV - open circuit voltage, R - internal resistance, Q_{max} - battery capacity):

$$\dot{SOC} = -\frac{OCV\left(SOC\right) - \sqrt{OCV\left(SOC\right)^2 - 4R\left(SOC\right) P_b}}{2R\left(SOC\right) Q_{max}} \quad (13)$$

where, for $pos \in \{crk, prim, sec, w\}$ the battery power is:

$$P_b = \sum_{pos} \frac{\pi}{30} \omega^{pos}_{EM} T^{pos}_{EM} + loss\left(\omega^{pos}_{EM}, T^{pos}_{EM}\right).$$

For a parallel architecture the component torques are independent and the rotational speeds directly determined from vehicle speed (exception for special cases of disconnection from the driveline). For a series-parallel architecture, the torque of an EM is calculated from the counterparts, but its speed is an additional degree of freedom, as in (1). Let:

$$L = \begin{bmatrix} r^w_{ICE} & r^{w/crk}_{EM} & r^{w/prim}_{EM} & r^{w/sec}_{EM} & rat^{w}_{EM} \end{bmatrix}$$

$$T_{EM} = \begin{bmatrix} T^{crk}_{EM} & T^{prim}_{EM} & T^{sec}_{EM} & T^{w}_{EM} \end{bmatrix}^T$$

$$\omega_{EM} = \begin{bmatrix} \omega^{crk}_{EM} & \omega^{prim}_{EM} & \omega^{sec}_{EM} & \omega^{w}_{EM} \end{bmatrix}^T$$

With these notations and by neglecting the terms in ω^{ctrl}_{ICE}, (3) can be reduced to a relation similar to (1):

$$T_w = L \begin{bmatrix} T_{ICE} \\ T_{EM} \end{bmatrix}, \begin{bmatrix} \omega_{ICE} \\ \omega_{EM} \end{bmatrix} = L^T \frac{v}{R_w} \quad (14)$$

Note that the proposed model can also describe the series architecture. In this case, the engine is decoupled from the drivetrain and there are two EM: one for traction, and another that acts as a generator, to convert the engine mechanical output into electricity. From Fig. 1 this implies: $C_1 = 0, C_2 = 0$, the traction motor is EM^{prim} and the generator- EM^{crk}. The engine and generator speed will be exclusively defined by ω^{ctrl}_{ICE} ($r^w_{ICE} = 0$).

The terms in matrices A_T and A_ω include products between the 2 clutches in order to appropriately integrate special use-cases of a DCT, as detailed in Table 3. For instance, (6) defines the ratio between the torque at primary and at crankshaft and it is the arithmetical expression for the logical OR operation. Equation (10) is detailed in Table 2, which is well defined for $rat^{prim}_{EM} \neq 0$. For a DCT, if both clutches are closed, the EM will run at the same speed as the ICE, the operating point being defined by the vehicle speed and the gear engaged on the odd shaft (R_1).

Table 2. EM to primary shaft, (10) description

C_1	C_2	$r^{sec/prim}_{EM} / rat^{prim}_{EM}$	Configuration
0	0	R_2	1, 2
0	1	R_2	1, 2, 3
1	0	R_2	2
1	1	R_1	2

The condition that ensures the engine is disconnected from the drive (its speed being therefore defined by ω^{ctrl}_{ICE}) is $C_1 + N_2 C_2 = 0$. This covers the cases where both clutches are open and also the charge at standstill mode ($C_1 = 0, C_2 = 1, N_2 = 0$). The latter is defined for an architecture with one EM to the primary shaft and involves decoupling the engine from the wheel ($N_2 = 0$) and closing the clutch between the engine and the EM^{prim} ($C_2 = 1$). In the case of a DCT, C_1 will be set to zero, according to assumption (iii) from section 2. Thus, the EM rotational speed will be equal to ω^{ctrl}_{ICE} and this is defined in the ω^{prim}_{EM} expression by the term $C_2\left(1 - C_1\right)\left(1 - N_2\right)$.

2.3 Case-study: hybrid architecture with a DCT

In this section, a DCT hybrid architecture is considered, with one EM connected to the primary shaft. This configuration allows both clutches to be simultanously closed in same particular cases: take-off and charge during driving, in parallel mode (the ICE and EM run at the same speed). In this case, the even shaft must be decoupled from the wheel ($R_2 = 0$). The table 3 summarizes the use-cases with respect to clutch states and even shaft (coupled/decoupled).

Table 3. Hybrid DCT functional modes

C_1	C_2	N_2	*Case*
0	0	0	standstill, sailing
0	0	1	electric driving, regenerative braking
0	1	1	hybrid or conventional, even gear engaged
0	1	0	charge during standstill
1	0	0	conventional driving, odd gear engaged
1	0	1	hybrid driving
1	1	0	take-off, charge during driving (parallel mode)

The charge during driving case can appear under 2 forms: torque split and parallel mode, as presented in Fig. 4. In

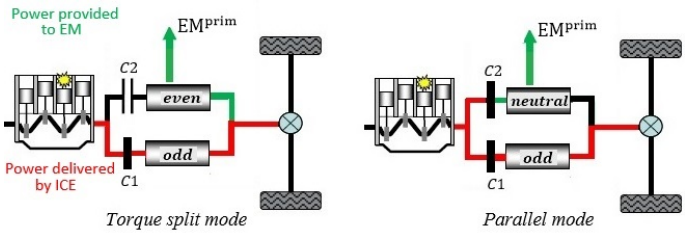

Fig. 4. Charge during driving: torque split and parallel mode

the first mode, the EM uses an even gear to provide generator torque, while ICE delivers positive torque through either sub-transmission. In the second, both clutches are closed and the 2 components run at the same speed, determined by the vehicle velocity and the odd gear engaged.

3. ENERGY MANAGEMENT - PROBLEM FORMULATION AND RESULTS

In this section, the energy management problem will be addressed and it will be shown how the model introduced in the previous section can be exploited for its formulation. The main objective for the design point of view is the fuel consumption minimization which requires a torque distribution between the ICE and the EM. Fuel consumption is given by a nonlinear static map, as a function of engine torque and speed, but for control design, an analytical approximation is employed. In de Jager et al. (2013) a convex model is proposed for the consumption of an SI engine:

$$P_f(\omega, P_p) = \gamma_{p,0} + \gamma_{p,1} P_p + \gamma_{p,2} P_p^2; \gamma_{p,2} \geq 0, \quad (15)$$

where P_p is the engine power. In the present paper, 3 alternative polynomial formulations (16a)-(16c) are introduced, which are compared to an approximation directly resulting from (15). The coefficients $p_i, i = 0 \dots 2$ are interpolated values and $\dot{m}_f$ is the instantanous fuel consumption:

$$\dot{m}_f = p_1(\omega_{ICE}) T_{ICE} + p_0(\omega_{ICE}) \quad (16a)$$

$$\dot{m}_f = p_2(\omega_{ICE}) T_{ICE}^2 + p_1(\omega_{ICE}) T_{ICE} + p_0(\omega_{ICE}) \quad (16b)$$

$$\dot{m}_f = p_2(T_{ICE}) \omega_{ICE}^2 + p_1(T_{ICE}) \omega_{ICE} + p_0(T_{ICE}) \quad (16c)$$

$$\dot{m}_f = \gamma_2 P_p^2 + \gamma_1 P_p + \gamma_{0,2} \omega_{ICE}^2 + \gamma_{0,1} \omega_{ICE} + \gamma_{0,0} \quad (16d)$$

Fuel consumption minimization favors an explicit relation in engine torque, as in (16a), (16b) or (16d). However, these approximations are less accurate than relation (16c), as can be seen in Table 4 where the RMSE (*Root Mean Square Error*) associated to validation data are summarized for a SI and CI engine, respectively, and also in Table 5, where the RMSE was calculated for different driving cycles (for the CI engine, only data for NEDC are available). The polynomial (16c) was therefore used, as it was validated with the best results for all the cases, with the remark that for the CI engine the polynomials in torque are also accurate.

As can be seen in Fig. 5, the torque dependence of the polynomial parameters in (16c) is highly nonlinear, but a piecewise linear approximation is possible (the curves in red) whose accuracy is quantified in the last column of

Table 4. RMSE for different consumption approximations [g/s] and average $\overline{\dot{m}_f}$.Validation on identification data

Engine	$\overline{\dot{m}_f}$	(16a)	(16b)	**(16c)**	(16d)
SI	2.67	0.75	0.5	**0.37**	0.6
CI	1.16	0.08	0.07	**0.06**	0.09

Table 5. RMSE for different fuel consumption approximations [g/s] and average $\overline{\dot{m}_f}$. Validation on drive cycles

Cycle/ICE	$\overline{\dot{m}_f}$	(16a)	(16b)	**(16c)**	(16d)	(17)
Road/SI	1.4	0.18	0.13	**0.08**	0.19	0.09
Urban/SI	1.39	0.13	0.09	**0.06**	0.18	0.07
High/SI	2.53	0.36	0.36	**0.07**	0.31	0.09
FTP/SI	1.28	0.11	0.09	**0.03**	0.16	0.04
NEDC/SI	1	0.12	0.04	**0.02**	0.13	0.04
NEDC/CI	0.33	0.02	0.02	**0.01**	0.03	0.015

Table 5. This approximation leads to a simplified version of (16c):

$$\begin{aligned} \dot{m}_f &= \left(a_2^{(i)} \omega_{ICE}^2 + a_1^{(i)} \omega_{ICE} + a_0^{(i)}\right) T_{ICE} \\ &+ b_2^{(i)} \omega_{ICE}^2 + b_1^{(i)} \omega_{ICE} + b_0^{(i)} \\ &\text{where} \quad p_j = a_j^{(i)} T_{ICE} + b_j^{(i)}, j = 0 \dots 2 \\ &T_{ICE}^{min(i)} \leq T_{ICE} \leq T_{ICE}^{max(i)}, i = 1 \dots N_{part} \end{aligned} \quad (17)$$

where N_{part} is the number of piecewise linear partitions (for the specific case considered here: $N_{part} = 5$).

The optimization criterion was chosen such that its expression includes the trade-off between the use of the 2 power sources, similar to ECMS. Due to convexity requirements and considering the expression for the fuel consumption approximation a weighted sum of the square of the two powers was used:

$$\min \sum_{i=k}^{k+N-1} P_f^2(i) + \lambda P_e^2(i) \quad (18)$$

and by detailing the terms, it can be expressed as:

$$\min \sum_{i=k}^{k+N-1} \dot{m}_f^2(i) + \lambda \left(\frac{1}{H_{LV}} Q_{max} OCV(k) S\dot{O}C(i)\right)^2 \quad (19)$$

where k is the current step, N is the prediction horizon, H_{LV} is the lower heating value of the fuel and SOC variation is given by (13). Another quadratic criterion is currently under study, where the electrical consumption is expressed by the difference between the electrochemical power and its minimal value, defined by constraints.This new criterion takes into account cases where P_e is negative.

For a charge-sustaining operation mode, a particular attention must be paid to the SOC balance. This could be ensured by choosing appropriate values for the penalty factor λ, but it is cycle-dependent (which is in turn characterized by speed profile and total duration). In this paper, distance-varying min-max limits for SOC were used:

$$\begin{aligned} SOC_{min}(k) &= SOC_0 - (SOC_0 - SOC_{min})\, e^{1 - \frac{1}{1 - \frac{dist(k)}{distTot}}} \\ SOC_{max}(k) &= SOC_0 + (SOC_{max} - SOC_0)\, e^{1 - \frac{1}{1 - \frac{dist(k)}{distTot}}} \end{aligned} \quad (20)$$

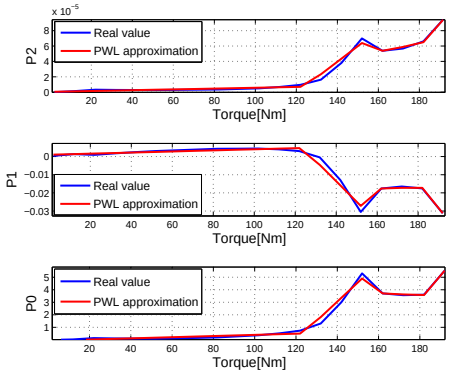

Fig. 5. Torque dependence of polynomial parameters; real values and PWL approximation

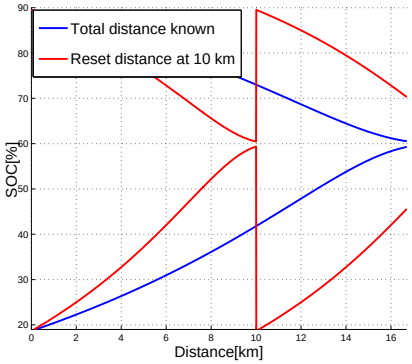

Fig. 6. SOC limits for 2 cases: total distance known and reset distance fixed at 10 km, respectively

The idea is to constrain SOC to gradually approach its initial value as the ratio between the actual distance and the total distance increases and, at the same time, allowing it a wide range of variation in the first part of the trajectory (SOC_{min}, SOC_{max} represent the physical limitations of the battery which were set at 20% and 90%, respectively). A final SOC equal to the initial value is especially useful in simulation, in order to make a fair comparison with a conventional vehicle or between different strategies. In practice, this constraint can be relaxed as we are only interested in maintaining SOC within a certain range (in average). Hence, when the total distance value is not available, the constraints are reset after a certain pre-defined distance. In simulation, it can be set to 5 or 10 km, but in real-driving situations this value could be chosen with respect to history data.

3.1 MPC formulation

The model-based predictive control strategy involves the resolution of a finite-time horizon optimization problem, at each time instant k:

$$\min_{\Delta u} \sum_{i=1}^{N} \left(\Delta x_{k+i}^T Q \Delta x_{k+i} + \Delta u_{k+i-1}^T R \Delta u_{k+i-1} \right) \tag{21a}$$

$$\text{s.t.} \begin{cases} x_{min} \leq x_{k+i} \leq x_{max}, & i = 1, ..., N \\ u_{min} \leq u_{k+i-1} \leq u_{max}, & i = 1, ..., N \end{cases} \tag{21b}$$

The problem is reformulated as a quadratic programming, where U represents the vector of future commands:

$$\min_{U \quad H>0} \quad \frac{1}{2} U^T H U + F^T U \tag{22a}$$

$$\text{s.t.} \begin{cases} A_{ineq} U \leq b_{ineq} \\ A_{eq} U = b_{eq} \end{cases} \tag{22b}$$

In our case, the only state variable is SOC whose model (13) is nonlinear; in Cairano et al. (2011), Feng et al. (2015) a simplified linear model was used, but for a NiMh battery, whose operating range was restricted to a narrow interval: 40%-60%. However, outside this range, the model is no longer valid. Here, a linearization at the operating point is performed, under the assumption that open circuit voltage and internal resistance are constant during the prediction. A Linear Time Varying (LTV) system is obtained:

$$x_{k+1} = A_k x_k + B_k u_k + D_k \tag{23}$$

where $x = SOC, A_k = 1, u_k = T_{ICE}(k)$ and D_k is a residual term due to linearization. It can be noticed that A_k is constant, which reflects the integral behavior of SOC. The model complexity is given by the time-variance of B_k and D_k, which depend on EM rotational speed and torque demand. After linear algebra manipulations, we have:

$$X_k = \Phi_k x_k + \Psi_k U_k + V_k \tag{24a}$$

$$\Phi_k(i) = ones(N, 1), \Psi_k(i, j) = \begin{cases} B_{k+j-1} & j \leq i \\ 0 & \text{else} \end{cases}$$

$$V_k^T = \begin{bmatrix} D_k & D_k + D_{k+1} & \dots & \sum_{i=1}^{N} D_{k+i-1} \end{bmatrix} \tag{24b}$$

where x_k is the SOC value at instant k and X_k, U_k the vectors of future states and commands, respectively.

As in (19), ΔSOC has to appear in an explicit form:

$$\Delta X_k = D_\Delta \left(\Phi_k x_k + \Psi_k U_k + V_k \right) + X_{k0} \tag{25a}$$

$$X_{k0} = \begin{bmatrix} x_k \\ \vdots \\ 0 \end{bmatrix}, \quad D_\Delta(i, j) = \begin{cases} -1 & i = j \\ 1 & i = j + 1 \\ 0 & \text{else} \end{cases} \tag{25b}$$

From (17), we have:

$$\dot{m}_f = \alpha(\omega_{ICE}) T_{ICE} + \beta(\omega_{ICE}) \tag{26}$$

Therefore, the optimization criterion (18) is reduced to a quadratic formulation as in (22), where the positivity requirement is always verified:

$$H = \Psi_k^T D_\Delta^T Q D_\Delta \Psi_k + \bar{\alpha}^2 \tag{27a}$$

$$F = \Psi_k^T D_\Delta^T Q \left(D_\Delta \left(\Phi x_k + V_k \right) + X_{k0} \right) + \bar{\alpha} \bar{\beta} \tag{27b}$$

with $\bar{\alpha} = diag\left(\alpha\left(\omega_{ICE,k+i-1}\right)\right), \bar{\beta}(i) = \beta\left(\omega_{ICE,k+i-1}\right)$ and $Q = diag\left(\lambda \left(\frac{1}{H_{LV}} Q_{max} OCV\right)^2\right)$. Future vehicle reference speed and gear engaged are considered known for the next N s and therefore, from (3) and (5) we can determine the rotational speeds for ICE and EM:

$$\omega_{ICE} = r_{ICE}^w \frac{v}{R_w} + (1 - C_1 - N_2 C_2) \omega_{ICE}^{ctrl} \tag{28a}$$

$$\omega_{EM}^{prim} = r_{EM}^{w/prim} \frac{v}{R_w} + rat_{EM}^{prim} C_2 (1 - C_1)(1 - N_2) \omega_{ICE}^{ctrl} \tag{28b}$$

The rotational speeds establish the torque and power constraints for each prediction step that can be easily

expressed from (2), whereas SOC constraints (20) are imposed from (24a):

$$T_{ICE} = \frac{T_w - r^w_{EM} T_{EM}}{r^w_{ICE}} \tag{29a}$$

$$T^{min}_{ICE}(\omega_{ICE}) \leq T_{ICE} \leq T^{max}_{ICE}(\omega_{ICE}) \tag{29b}$$

$$T^{min}_{EM}(\omega_{EM}) \leq T_{EM} \leq T^{max}_{EM}(\omega_{EM}) \tag{29c}$$

$$P^{min}_{EM}(\omega_{EM}) \leq \frac{\pi}{30}\omega_{EM} T_{EM} \leq P^{max}_{EM}(\omega_{EM}) \tag{29d}$$

$$SOC^{(k)}_{min} - \epsilon_k \leq X_k \leq SOC^{(k)}_{max} + \epsilon_k \tag{29e}$$

where the superscript *prim* was neglected, due to the presence of a single EM and ϵ_k are slack variables. All the studied driving cycles have power requirements achievable with the conventional mode (ICE only), so torque and power limitations can be imposed as hard constraints, without affecting the recursive feasibility of the receding horizon optimization. On the contrary, in the case of distance-varying SOC limitations, infeasibility might occur, especially toward the reset distance, where there is a narrow range of variation. These limitations are therefore included as soft constraints.

3.2 Simulation and results

The control law was tested under Matlab/Simulink and the behavior of the vehicle was simulated by a high-fidelity model, designed in AMEsim. The total distance was considered known *a priori* and a prediction horizon $N = 5s$ was used. The results are summarized in Table 6, where the comparison is made with the consumption in conventional mode; in the case of a final SOC value different from the initial one, a consumption correction was performed. For all the scenarios the control parameters are the same. It can be seen that the hybrid vehicle with a MPC strategy offers a consumption gain up to 26%.

Table 6. Fuel consumption [L/100 km] for different drive cycles; ICE-only without stop & start vs MPC for HEV

Cycle	Conventional	Hybrid	Gain
ARTEMIS road	5.8	5.32	8.2%
ARTEMIS urban	9.38	6.9	26.4%
ARTEMIS highway	8.2	8.01	2.3%
FTP-75	6.22	5.28	15.1%
NEDC	5.76	5.01	13%

4. CONCLUSIONS AND OUTLOOK

A generic parameterization under certain assumptions has been proposed for a hybrid powertrain, with detailed expressions for series and parallel architectures. For the energy management part, an MPC - based strategy has been presented and validated in simulation (Matlab and AMEsim) on a hybrid DCT case study. Current simulations show that encouraging results can be obtained with a MPC strategy. The quadratic formulation is still under investigation. In addition, a sensitivity analysis with respect to driver behavior and to tuning parameters (prediction horizon, penalty factor, reset distance), as well as a stability analysis will be the object of a future study.

REFERENCES

Borhan, H., A.Vahidi, Phillips, A., Kuang, M., Kolmanovsky, I., and Cairano, S.D. (2012). Mpc-based energy management of a power-split hybrid electric vehicle. *IEEE Transactions on Control Systems Technology*, 20, No. 3.

Cairano, S.D., Liang, W., Kolmanosky, I., Kuang, M., and Phillips, A. (2011). Engine power smoothing energy management strategy for a series hybrid electric vehicle. *American Control Conference*.

Chen, K., Bouscayrol, A., Berthon, A., Delarue, P., Hissel, D., and Trigui, R. (2009). Global modeling of different vehicles. *IEEE Vehicular Technology Magazine*.

de Jager, B., van Keulen, T., and Kessels, J. (2013). *Optimal control of hybrid vehicles, Advances in industrial control*. Springer.

Feng, L., Cheng, M., and Chen, B. (2015). Predictive control of a power-split hev with fuel consumption and soc estimation. *SAE Technical Paper*, 2015-01-1161.

Goerke, D., Bargende, M., Keller, U., Ruzicka, N., and Schmiedler, S. (2015). Optimal control based calibration of rule-based energy management for parallel hybrid electric vehicles. *SAE Technical Paper*, 2015-01-1220.

Guzzella, L. and Sciarretta, A. (2007). *Vehicle Propulsion Systems*. Springer, 2nd edition.

Josevski, M. and Abel, D. (2014). Energy management of a parallel hybrid electric vehicle based on stochastic model predictive control. *19th World Congress, The International Federation of Automatic Control*.

Kim, T., Manzie, C., and Watson, H. (2008). Fuel economy benefits of look-ahead capability in a mild hybrid configuration. *Proceedings of the 17th World Congress The International Federation of Automatic Control*.

Lu, Z., Song, J., Yuan, H., and Shen, L. (2013). Mpc based torque distribution strategy for energy management of power-split hybrid electric vehicles. *Proceedings of the 32nd Chinese Control Conference*.

Manzie, C., Kim, T., and Sharma, R. (2012). Optimal use of telemetry by parallel hybrid vehicles in urban driving. *Elsevier, Transportation Research Part C 25*.

Musardo, C., Rizzoni, G., Guezennec, Y., and Staccia, B. (2005). A-ecms: an adaptive algorithm for hybrid electric vehicle energy management. *European Journal of Control*.

Ripaccioli, G., Bernardini, D., Cairano, S., Bemporad, A., and Kolmanovsky, I. (2010). A stochastic mpc approach for series hybrid electric vehicle power management. *American Control Conference*.

Rizzoni, G., Guzzella, L., and Baumann, B. (1999). Unified modeling of hybrid electric vehicle drivetrains. *IEEE/ASME Transactions on Mechatronics*, 4, No 2.

Sciaretta, A., Back, M., and Guzzella, L. (2004). Optimal control of parallel hybrid electric vehicles. *IEEE Transactions on Control Systems Technology*, 12, No 3.

Sciarretta, A., Guzzella, L., and Back, M. (2004). A real-time optimal control strategy for parallel hybrid vehicles with on-board estimation of the control parameters. *Proc. IFAC Symp. Adv. Automotive Control*.

Sundstrom, O., Guzzella, L., and Soltic, P. (2008). Optimal hybridization in two parallel hybrid electric vehicles using dynamic programming. *Proc. of the 17th World Congress IFAC*.